Environ. Sci. Technol. **2001**, *35,* 1531−1536

Effect of Electric Arc Vitrification of Bottom Ash on the Mobility and Fate of Metals

HOLGER ECKE,*,† HIROFUMI SAKANAKURA,‡,§ TOSHIHIKO MATSUTO,‡ NOBUTOSHI TANAKA,‡ AND ANDERS LAGERKVIST†

Division of Waste Science and Technology, Luleå University of Technology, SE-971 87 Luleå, Sweden, and Department of Environmental and Sanitary Engineering, Hokkaido University, Kita 13 Nishi 8, Kita-ku, Sapporo 060-0813, Japan

Increasing amounts of municipal solid waste incineration (MSWI) residues are treated prior to landfilling or reuse. In Japan, electric arc melting is used for bottom ash vitrification that generates a glasslike slag. The objective of this paper was to assess this pretreatment technique with respect to its effect on metal mobility and metal content. Both bottom ash and slag were sampled and analyzed on total solids (TS), fixed solids (FS), particle density (ρ_P), specific BET surface area, particle size distribution, and total element content. A six-step wet sequential extraction procedure was used for assessing metal mobility. The results were qualitatively verified by scanning electron microscopy. The major conclusion was that the availability of various metals was affected differently by electric arc vitrification. Metals were solidified, stabilized, and/or separated from the slag. The mobility of Cr, Cu, Zn, Pb, and Ca was reduced. In slag, major fractions of these elements were found in moderately reducible phases or in the residual slag lattice. The approximately three-fourths of Pb [174 ± 7 mg (kg of FS)$^{-1}$] and half of Zn content [676 ± 352 mg (kg of FS)$^{-1}$] were most likely removed from bottom ash through evaporation. The total content increases of Al, Cr, Ni, and Cd (51 ± 3, 621 ± 27, 138 ± 19, and 99 ± 32%, respectively) were probably caused by the wear of furnace refractories.

Introduction

In many industrialized countries incineration has become a widely used treatment technique for municipal solid waste (MSW); for example, in Sweden ∼55% of the MSW is incinerated (*1*). Worldwide, Japan has the highest ratio of MSW incineration with ∼74% (*2*) operating in ∼1854 plants with a total capacity of 1.78×10^5 tons day^{-1} (*3*). Solid residues from municipal solid waste incineration (MSWI) are bottom ash and air pollution control (APC) residues. Both waste streams pose particular environmental threats due to the risk of releasing toxic organic compounds and metals. To cope with this problem, Japan's Waste Disposal and Public Cleansing Law stipulates for all incinerators with a capacity ≥5 tons day^{-1} that APC residues must not be disposed of unless they are treated to immobilize environmentally relevant metals. Today, bottom ash treatment is also being applied.

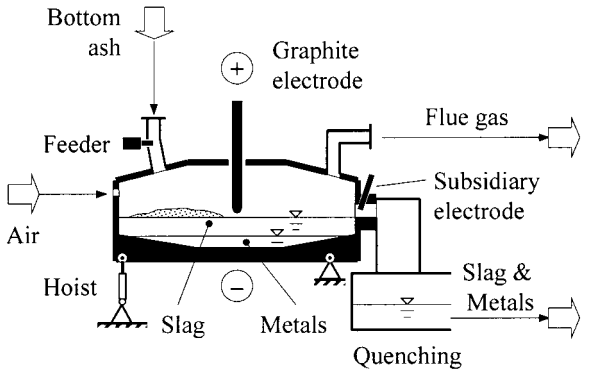

FIGURE 1. Electric arc furnace used for bottom ash melting at an MSW incinerator in Saitama prefecture near Tokyo, Japan (adopted from ref *5*).

An acceptable treatment technique is melting, which includes electric, burner, and blast melting. Thermal processing of MSWI residues gains some advantages over other treatment options; namely, it leads to a volume reduction, a destruction of >95% of dioxins (as toxicity equivalents, TEQ) (*4*), and metals can be separated in some types of melting furnaces by evaporation or phase separation (*5*). It is also expected that compared to nontreated residues, molten MSWI ashes have a much lower potential to mobilize metals. However, the latter aspect has not been thoroughly investigated. In Japan, the total melting capacity amounts to ∼1500 tons day^{-1}, of which one-third is based on electric arc melting (*5*).

It was attempted in this investigation to understand the effect of electric arc vitrification of bottom ash with respect to the mobility of metals. We were also aiming to quantify metal fluxes over an electric arc furnace.

Experimental Section

Material. At an MSW incinerator in Saitama prefecture near Tokyo, Japan, bottom ash is treated by a sequence of crushing, magnetic separation, drying in a rotary dryer, electric arc melting, and quenching. The ash melting system consists of two electric arc furnaces (Figure 1) with a capacity of 80 tons day^{-1} each. Melting is carried out using direct current and graphite anodes as well as a sump of separated metals as cathodes. The graphite electrode is controlled above the melt to build up a stable electric arc. Gravimetric separation of metals from the slag leads to sump formation. Feeding and tapping are carried out sequentially. Both the slag and sump are tapped simultaneously and quenched with water. The product is called slag; that is, it includes metal phases from the sump. A subsidiary electrode at the tap hole of the furnace removes pluggings. The following feedstock quality is usually required: water content, <5%; unburned content, <3%; metal content, <20%; and ash size, <100 mm (*6*). During operation, the furnace atmosphere is oxidizing from 1000 to 1300 °C. Arc plasma is controlled at a temperature of between 3000 and 5000 °C, whereas the molten bath is from 1300 to 1500 °C. For each ton of bottom ash, the power input supplied by the incinerator is from 550 to 800 kWh, the electrode wear is ∼6−10 kg, and the generation of flue dust is ∼0.04 tons.

* Corresponding author phone: +46-920-720 41; fax: +46-920-914 68; e-mail: Holger.Ecke@sb.luth.se.
† Luleå University of Technology.
‡ Hokkaido University.
§ Present address: Division of Civil and Environmental Engineering, Akita National College of Technology, 1-1 Bunkyocho Iijima, Akita 011-8511, Japan.

10.1021/es0001759 CCC: $20.00
Published on Web 03/06/2001

TABLE 1. Estimation of Metal Bonds in the Six Fractions of the Sequential Extraction Procedure and the Respective Extraction Reagents

extraction step	reagant	fraction
I	1 M ammonium acetate	exchangeable cations
II	1 M sodium acetate	carbonates
III	0.1 M hydroxylammonium chloride	easily reducible phases (manganese oxide, amorphous iron oxide)
IV	0.2 M ammonium oxalate and 0.2 M oxalic acid	moderatley reducible phases (amorphous and poorly crystallized iron oxide)
V	hydrogen peroxide, 30%	metals bound to organic matter and sulfides
VI	aqua regia and hydrofluoric acid	residuals (e.g., silicates, crystalline iron oxide)

Furnace refractories are subjected to wear and have to be regularly renewed. Total volume of bottom ash reduction achieves ~20%. The plant started operation in October 1995.

During one week of regular plant operation, sampling was performed three times. Bottom ash was taken after magnetic separation and slag after quenching. The three fractions of each material were mixed, and 10 kg was used for further quartering in the laboratory.

Analytical Methods and Apparatus. The following analytical methods were applied on both bottom ash and slag samples.

The total solid content (TS) was determined according to the Swedish standard for wastewater sludge (*7*); that is, ~50 g of sample was dried at 105 °C for 24 h.

Two different temperatures were used for fixed solid (FS) analyses. FS_{550} was determined at a glowing temperature of 550 °C and FS_{775} at 775 °C. The former corresponds to the Swedish standard for wastewater sludge (*7*).

The particle density (ρ_P) was determined using a helium pycnometer (Micromeritics multivolume pycnometer 1305).

A BET surface area analyzer (Micromeritics FlowSorb II 2300) was used to determine the specific surface area.

Dry sieving was applied for investigating the particle size distribution (*8*). Sample classification was performed using the Unified Classification System (*9*). The underlying geotechnical properties were the uniformity coefficient (C_u), the coefficient of curvature (C_z), and the weight percentage passing a no. 200 sieve (F_{200}), which corresponds to a sieve opening of 0.075 mm. C_u and C_z are defined as

$$C_u = D_{60}/D_{10} \quad (1)$$

and

$$C_z = D_{30}^2/(D_{60}D_{10}) \quad (2)$$

where D_{10}, D_{30}, and D_{60} are the particle diameters (d) corresponding to the percentages finer than 10, 30, and 60%, respectively.

Total decomposition was performed with 1 g of sample gently boiled in 40 mL of aqua regia for 3 days.

To assess metal mobility, a wet sequential extraction procedure in six leaching steps was adopted (*10*). Using ~0.5 g dry weight of a sample, metal fractionation was achieved by applying extraction conditions in increasing order of strength. The first leaching step was performed in an anaerobic environment at neutral pH. In the following steps, the pH was successively lowered while the redox potential was shifted to oxidizing conditions. The extraction scheme partitioned the samples into six element fractions with increasing binding strengths, thus indicating the availability of the metals (Table 1).

Elemental analyses were performed using inductively coupled plasma mass spectrometry (ICP-MS) (Hewlett-Packard HP4500).

Scanning electron microscopy (SEM) (Hitachi S-3200N scanning electron microscope) was used to qualitatively examine and compare the untreated and extracted samples. All SEM specimens were dried at 60 °C, mounted on a metal stub, and coated with Pt using a Hitachi E-1030 mild ion sputter coater.

Statistics. The *F* test was used to compare variances and the *t* test to compare averages (*11*). Error propagation was calculated using the spreadsheet method (*12*).

TABLE 2. Average with Standard Deviation (SD) ($n = 3$) of the Particle Density (ρ_P), Mass-Specific BET Surface (BET_{spec}), and Volume-Specific Surface Area

	ρ_P (g cm^{-3})		BET_{spec} (m^2 g^{-1})		$\rho_P \times BET_{spec}$ (m^2 cm^{-3})	
sample	av	SD	av	SD	av	SD
bottom ash	2.44	±0.01	6.37	±0.05	15.54	±0.14
slag	2.83	±0.01	0.68	±0.03	1.92	±0.10

[a] The volume-specific surface area is calculated from the particle density and the mass-specific BET surface by taking into account error propagation.

Results and Discussion

Electric arc vitrification comprises three different approaches to treat metals, namely, solidification, stabilization, and separation. In the following, we present the change in physical properties due to electric arc vitrification and discuss the effect on solidification. Both metal stabilization and metal separation, in the second and third sections, are estimated by comparing the chemical properties of bottom ash and slag. By means of topographical investigations, the conclusions are qualitatively verified.

Physical Properties. Solidification is achieved by physical binding such as micro- or macroencapsulation (*1*). Electric arc vitrification significantly increased the potential for physical binding. Compared with bottom ash, slag had a 1 order of magnitude lower mass specific surface area (Table 2). Taking error propagation and the change in particle density into account, the volume-specific surface area yielded 15.54 ± 0.14 m^2 cm^{-3} for bottom ash and 1.92 ± 0.10 m^2 cm^{-3} for slag. Although 80 wt % of the slag consisted of particles smaller than bottom ash (Figure 2), slag had a specific surface area ~10 times smaller than bottom ash. This indicates that slag had a much smoother surface. For bottom ash, $C_u/C_z/F_{200}$ were 14/1.5/<5, and for slag, 2.9/1.2/<5. This corresponds to *well-graded sand* ($C_u \geq 6$, $1 \leq C_z \leq 3$, $F_{200} < 5$) for bottom ash and to *poorly graded sand* ($C_u < 6$ and/or C_z not between 1 and 3, $F_{200} < 5$) for slag (*9*).

Mobility of Metals. Vitrification of bottom ash leads to a chemically restructured waste matrix having the potential to stabilize metals (*1*). The amorphous, glasslike matrix of slag is composed of the abundant elements Si, O, Al, and Ca (*13*). The results from the sequential extraction (Figure 3) confirmed phase changes especially for Ca. In slag, 98 ± 3% of Ca was found in the residual glassy matrix (sequential extraction step VI), whereas in bottom ash, Ca was shared among the exchangeable cation fraction (38 ± 2%) (step I),

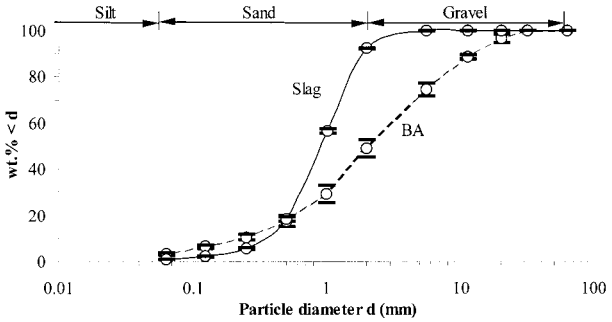

FIGURE 2. Particle-size distribution of bottom ash and slag with averages (○) and standard deviations (−) ($n = 3$). Size limits for silt, sand, and gravel were as recommended by MIT (*9*).

the carbonate fraction (24 ± 1%) (step II), and the residual fraction (33 ± 10%).

It was also shown that Cu was effectively retained in the slag matrix. Vitrification increased the percentage of Cu bound in the extraction step VI from 28 ± 5 to 89 ± 8%.

In the slag, we detected Cr predominantly in moderately reducible phases (37 ± 1%) and in the residual waste matrix (61 ± 2%). Compared with bottom ash, Cr was less available in extraction steps I−III and V. From an environmental point of view, the lowered availability in the first three steps is important. It indicated that easily reducible (*14*) and mobile hexavalent chromium [Cr(VI)] was reduced to the trivalent oxidation state [Cr(III)], which forms a large number of kinetically inert complexes (*14*). Whereas Cr(VI) is classified as a pollutant causing cancer, mutations, and allergies, compounds of Cr(III) are much less toxic (*14*, *15*). In the natural environment, a reoxidation of reduced Cr is very unlikely (*16*, *17*). Kersten et al. (*18*) investigated the importance of Cr(VI) in leachates from bottom ash monofills and found that Cr(VI) is the dominating species. This finding contributes to the environmental significance of electric arc vitrification.

A reduced availability in the first three extraction steps was also observed for Zn.

Bottom ash liberated about one-third of the total Pb content in the carbonate fraction (step II). However, carbonates are thermally decomposed under melting conditions; therefore, the slag fixed Pb predominantly in the residual glassy matrix.

In contrast to the above elements, the availability of Al was not significantly reduced with vitrification. In leaching step IV, almost half of the Al content was detached from the lattice of both bottom ash and slag; these fractions most likely represent aluminum silicates. First, the oxygen atom bridging Si and Al in aluminum silicates is sensitive to proton attack (*19*). Furthermore, Al detachment can be enhanced with ligands (*20*). Proton-promoted dissolution supported by ligand-promoted detachment is a characteristic feature of leaching step IV by applying oxalic acid and oxalate.

In bottom ash, Fe was almost equally bound either in moderately reducible phases or in the residuals. In slag, Fe dominated in extraction step VI. However, melting affected the overall mobility of Fe only slightly. The extraction pattern of Ni was similar to that of Fe.

Thermal treatment seemed to have no effect on the mobility of Cd. This element was detected at similar concentrations in the corresponding fractions of both materials.

We found that the melting of bottom ash reduced the availability of elements such as Cr, Cu, Zn, Pb, and Ca, whereas the mobility of Cd, Al, Fe, and Ni was barely affected. Slag was stable to chemical attack as established under extraction steps I−III. In moderately reducible phases (step IV), we observed significant proportions of Al, Cr, Fe, and

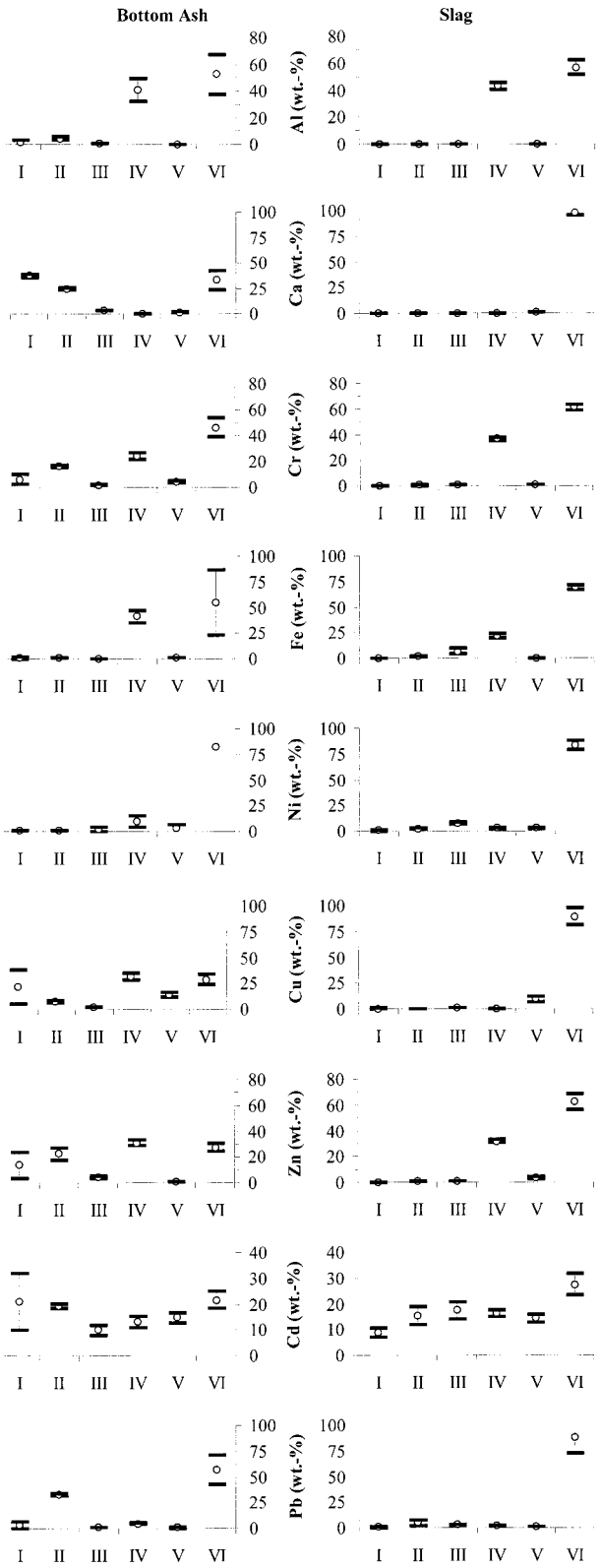

FIGURE 3. Weight percentages of Al, Ca, Cr, Fe, Ni, Cu, Zn, Cd, and Pb mobilized in the corresponding leaching step of the sequential extraction procedure. Diagrams on the left (bottom ash) and on the right (slag) show averages (○) and standard deviations (−) ($n = 3$).

Zn. Bottom ash was less stable than slag with respect to the first two extraction steps. For both materials, the proportion of metals bound to easily reducible phases (step III) appeared to be low. With the exception of Cd and Cu, neither bottom

ash nor slag fixed >5 wt % of any metal to organic matter or sulfides (step VI).

With the sequential extraction procedure used, it was not possible to make statements about the material stability at alkaline conditions. Regarding the deposition or reuse of slag in natural environments, we assume that this aspect is of minor importance. Due to biological and/or chemical processes such as anaerobic degradation and carbonation under atmospheric carbon dioxide, pH is usually stabilized at levels below pH 9. Another investigation (*21*) indicates that the chemical stability of vitrified wastes is lowered at pH >10. Such extreme environments might enhance the alteration of the glassy phases of slag to clays. What has not yet been investigated is how this affects metal mobility.

To assess the mobility of metals in particulate matter such as sediment and waste, more than two dozen different sequential extraction protocols were developed (*22*). The selectivity of such procedures is questioned in several papers (*23*−*29*). A major issue addressed is redistribution, which reduces the validity of the speciation. However, other investigations (*22*, *30*−*34*) indicate sufficient precision and accuracy as well as usefulness of sequential extractions. It might not be possible to draw general conclusions due to the differences in sequential extraction protocols and the characteristics of the particulate matter under investigation. In this work, we did not confirm the speciation results with other methods. Nevertheless, by using the applied procedure, we might estimate the impact of different environments on the mobility of operationally defined groups of metal forms and also associations from bottom ash compared with slag.

Alternatively, metal mobility can be assessed by extraction tests that are designed to make mechanistic models rather than operationally defined models, for instance, the dynamic leach test (*35*), which is used to determine the diffusion coefficients for contaminants, and the column test (*36*), used to assess in situ leaching behavior of wastes. Such tests usually resemble each other in that they are easy to perform. The disadvantage is that results are valid for only one setup of defined conditions. However, factors controlling metal mobility, for example, pH and redox potential, can vary significantly between different environments as well as over time. For some leaching protocols, the levels of such critical factors are not even defined.

The impact of electric arc vitrification was limited not only to solidification and stabilization. The treatment also affected the total element content as well as the homogeneity of bottom ash. This is shown in the following section.

Fate of Metals. Element fluxes over the electric arc furnace were quantified to assess the impact of vitrification on the fate of metals. Data from the total decomposition of bottom ash and slag (Figure 4) were statistically evaluated using the comparison of variances and averages ($n = 4$, $\alpha = 0.05$). As a reference representing the content of fixed solids, we chose FS_{775} because the glowing of bottom ash resulted in a 12 ± 9.3 g (kg of TS)$^{-1}$ higher loss of mass at 775 °C than at 550 °C (Table 3).

The difference in loss of mass might be due to the decomposition of carbonates, typically liberated at ~750 °C. A total carbonate content of ~12 g (kg of TS)$^{-1}$ in bottom ash seems to imply an inconsistency with the results from the sequential extraction. An amount of 12 g (kg of TS)$^{-1}$ of CO_3^{2-} has the potential to bind 8 g (kg of TS)$^{-1}$ of Ca; however, in leaching step II (carbonate phase), ~4-fold this amount of Ca was extracted. This raises the query as to whether (a) the carbonate content of bottom ash was underestimated because, for example, not all carbonates were decomposed at 775 °C or (b) in step II of the sequential extraction not only the carbonate phases were mobilized. Thermogravimetry might be useful to give a better resolution on the carbonate

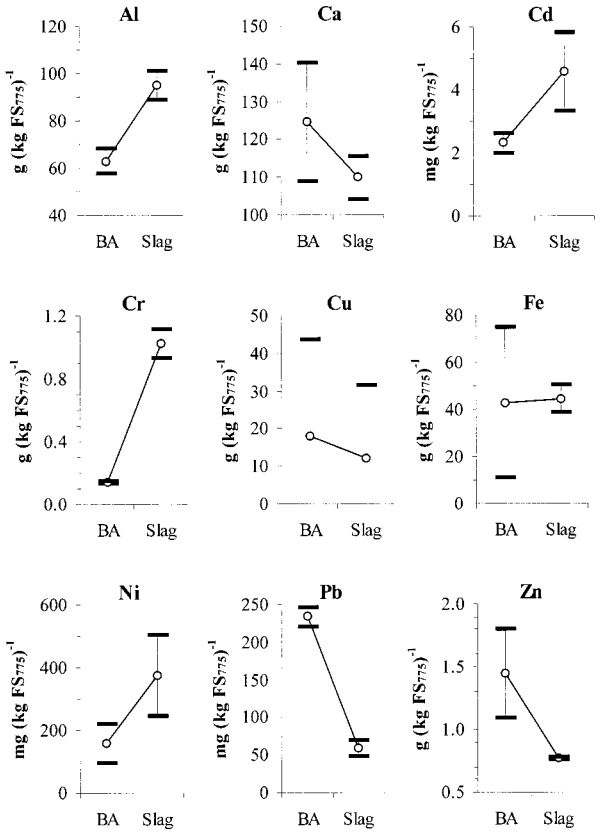

FIGURE 4. Averages (○) and standard deviations (−) ($n = 4$) for total element contents in bottom ash (BA) and slag. BA values were corrected for error propagation regarding variation in both concentration per TS and FS_{775}. For slag data, it was assumed that FS_{775} = 1.000 kg of FS (kg of TS)$^{-1}$.

TABLE 3. Average with Standard Deviation (SD) of the TS, FS_{550}, and FS_{775}

	TS[a] (g kg^{-1})		FS_{550}[b] [g (kg of TS)$^{-1}$]		FS_{775}[b] [g (kg of TS)$^{-1}$]	
sample	av	SD	av	SD	av	SD
bottom ash	682	±8.7	970	±7.6	958	±5.4
slag	971	±1.2	999	±0.3	1,001	±0.5

[a] $n = 3$. [b] $n = 5$.

content and may also bear the potential to distinguish between different metal carbonate phases.

A comparison of averages of total element contents showed that vitrification causes both depletion and enrichment of metals. Significant separation from bottom ash was observed for Pb and Zn. In slag, 25% of Pb [60 ± 10 mg (kg of FS_{775})$^{-1}$] and 53% of Zn [773 ± 9 mg (kg of FS_{775})$^{-1}$] were determined. During the melting process, these two metals most likely evaporated as flue dust from the molten bath because at 1300−1500 °C the boiling point of elemental Zn (907 °C) is exceeded and the boiling point of elemental Pb (1749 °C) is almost reached. Besides their elemental states, these elements were probably also present as chlorides having significantly lower boiling points, namely, 732 °C for $ZnCl_2$ and 950 °C for $PbCl_2$ (*37*). In bottom ash, the content of chlorides varies between 0.8 and 4.19 g (kg of TS)$^{-1}$ (*1*).

Contrarily, the net flux of Cd, Al, Cr, and Ni was significantly higher for slag than for bottom ash. The three latter elements are abundant in common furnace refractories composed of materials such as bauxite, mullite, chromium corundum, and Cr−Ni alloys. During furnace operation, the

refractory wears and its constituents are incorporated into the melt. This might explain an enrichment that yielded approximately 51 ± 3% for Al, 621 ± 27% for Cr, and 138 ± 19% for Ni. The flux of Cd was ~2-fold, that is, it increased from ~2.3 ± 0.3 to 4.6 ± 1.2 mg (kg of FS_{775})$^{-1}$. This observation was surprising because elemental Cd has a rather low boiling point of 767 °C (*37*) and a depletion as for Pb and Zn was expected. Crystalline CdO sublimes at 1559 °C (*37*), that is, greater than the operation temperature of the furnace. Under the oxidizing atmosphere, the formation of CdO was possible. However, even without any evaporation of Cd, the doubling of Cd content cannot be explained; a reason for this could be that Cd was also an admixture in the refractories. Unfortunately, the confirmation of the above hypothesis was impeded due to trade secrets protecting information about the composition of the refractories.

No significant difference in element content was observed for Ca, Cu, and Fe.

After total digestion, some solid residues remained undissolved; this involves a possible source of error for the metal contents discussed above. Because aqua regia may not completely dissolve aluminosilicate matrices, Al data should be considered as minimum content.

The working hypothesis that vitrification increases the homogeneity of the element content was tested by comparing variances. However, at a significance level of $\alpha = 0.05$, the hypothesis was confirmed only for Fe and Zn. Cd and Cr showed an even higher variation in slag than in bottom ash samples. This observation could be due to the segregation of the molten bottom ash into two phases during melting (Figure 1). Although both phases are tapped and quenched simultaneously, the metal-rich sump might not mingle completely with the rest of the bath.

Topographical Features. During the course of sequential leaching, the topographical feature of bottom ash and slag changed because of chemical attack (Figure 5).

Raw bottom ash was characterized by an uneven crystalline surface structure, whereas slag showed the rough-edged feature of a glasslike material. The bottom ash−water interface probably favored adsorption and desorption processes to a much higher extent than slag. Vitrification causing surface smoothing led to a lower specific surface area and, thus, the encapsulation of metals.

The crystalline feature of bottom ash disappeared with the first leaching in ammonium acetate. Crystals composed of, for example, Ca, might be restructured or dissolved. Comparing bottom ash with slag, the wear of the latter was less from leaching steps I−III. This is in agreement with the investigations on metal mobility. Slag appeared to be stable to chemical attack within the first three leaching steps. Ammonium acetate (leaching step I) removed most of the attached particles smaller than ~1 μm but did not attack the surface of the slag. Extraction with sodium acetate (step II) and hydroxylammonium chloride (step III) caused the first signs of wear, but most of the elements might be still encapsulated by the slag lattice. Severe decomposition was detected after leaching step IV. This coincides with a considerably increased availability of Al, Cr, Fe, and Zn.

Electric arc vitrification appeared to greatly affect metal availability. Environmentally relevant metals such as Cr, Cu, Zn, and Pb were removed from bottom ash and/or their mobility was significantly lowered. The present investigation proved that under moderate conditions, the risk of release of toxic metals was lower for slag than for bottom ash. This might justify the use of slag as a construction material, for example, as a subbase in road construction or supplement for pavement. However, an overall assessment of the melting technique has to take into account more aspects than are treated here, for example, the destruction of persistent organics. We did not characterize the metal-laden flue dust generated during melting. Due to the presence of mobile metal contaminants, this product might be highly toxic and might therefore require special treatment.

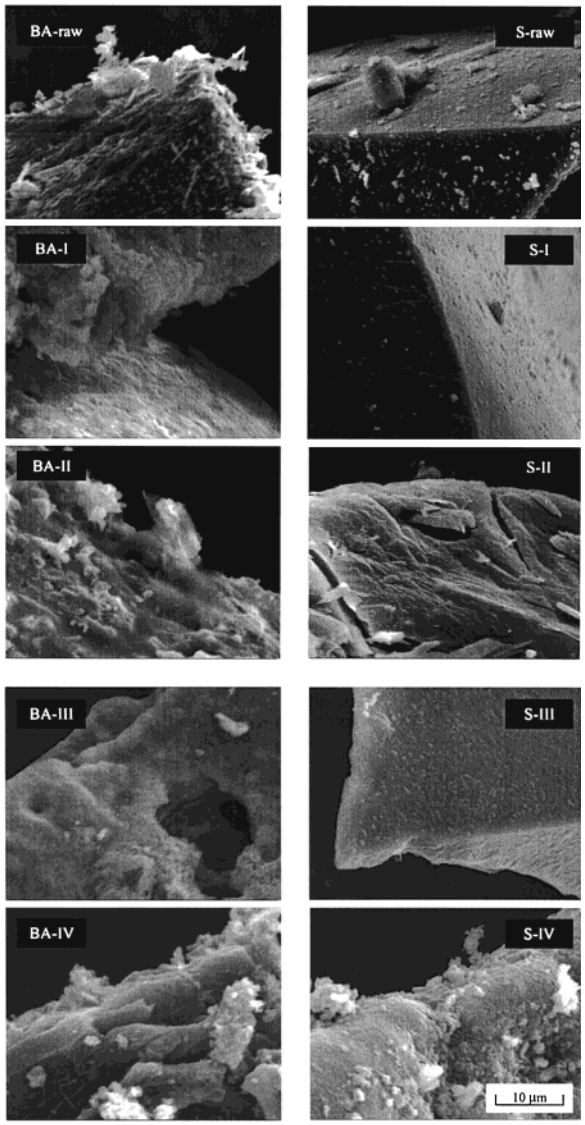

FIGURE 5. SEM images of the topographical feature of bottom ash (BA, left) and slag (S, right) and its changes due to sequential extraction until step IV. All images were taken with 20 kV acceleration voltage and identical magnification.

Acknowledgments

The financial support of the Swedish Institute, Stockholm, and the Board of Faculty at Luleå University of Technology, Sweden, is greatly acknowledged. We thank Rolf Sjöblom (ÅF, Sweden) for his valuable comments on the manuscript. Jorg Thöming (Universidade Federal do Rio Grande do Sul, Brazil) and Wolfgang Calmano (TU Hamburg−Harburg, Germany) provided welcome additional input.

Literature Cited

(1) Chandler, A. J.; Eighmy, T. T.; Hartlén, J.; Hjelmar, O.; Kosson, D. S.; Sawell, S. E.; van der Sloot, H. A.; Vehlow, J. *Municipal Solid Waste Incinerator Residues*; Elsevier Science Publishers: Amsterdam, The Netherlands, 1997.

(2) Sakai, S.; Sawell, S. E.; Chandler, A. J.; Eighmy, T. T.; Kosson, D. S.; Vehlow, J.; van der Sloot, H. A.; Hartlén, J.; Hjelmar, O. *Waste Manage.* **1996**, *16*, 341−50.

(3) Sambongi, T.; Hara, T.; Tanaka, M.; Ishii, A.; Doi, K.; Osako, M.; Osawa, T.; Asai, T.; Ishiguri, A.; Ishiawata, K.; Sakurai, K.;

Hashizume, H. *Waste Management in Japan 1996*; Japan Waste Management Association: Tokyo, Japan, 1996.
(4) Ito, T. *Waste Manage.* **1996**, *16*, 453−460.
(5) Ecke, H.; Sakanakura, H.; Matsuto, T.; Tanaka, N.; Lagerkvist, A. *Waste Manage. Res.* **2000**, *18*, 41−51.
(6) Kinto, K. *Waste Manage.* **1996**, *16*, 423−430.
(7) Swedish Institute for Standards, 1981; SS 02 81 13.
(8) Swedish Institute for Standards, 1992; SS 02 71 23.
(9) Das, B. M. *Principles of Foundation Engineering*, 2nd ed.; PWS-Kent: Boston, MA, 1990.
(10) Calmano, W.; Förstner, U. *Sci. Total Environ.* **1983**, 77−90.
(11) Miller, J. C.; Miller, J. N. *Statistics for Analytical Chemistry*, 3rd ed.; Ellis Horwood: Chichester, U.K., 1993.
(12) Kragten, J. *Analyst* **1994**, *119*, 2161−2165.
(13) Panne, U.; Clara, M.; Haisch, C.; Niessner, R. *Spectrochim. Acta, Part B* **1998**, *53*, 1969−1981.
(14) Moore, J. W.; Ramamoorthy, S. In *Heavy Metals in Natural Waters: Applied Monitoring and Impact Assessment*; Moore, J. W., Ramamoorthy, S., Eds.; Springer-Verlag: New York, 1984; Chapter 4.
(15) *IARC Monographs on the Evaluation of Carcinogenic Risks to Humans—Chromium, Nickel and Welding*; World Health Organization, International Agency for Research on Cancer: IARC: Lyon, France, 1990; Vol. 49.
(16) Losi, M. E.; Amrhein, C.; Frankenberger, W. T., Jr. *Environ. Toxicol. Chem.* **1994**, *13*, 1727−1735.
(17) Ohtake, H.; Silver, S. In *Biological Degradation and Bioremediation of Toxic Chemicals*, 1st ed.; Chaudhry, G. R., Ed.; Chapman & Hall: London, U.K., 1994; Chapter 19.
(18) Kersten, M.; Schulz-Dobrick, B.; Lichtensteiger, T.; Johnson, C. A. *Environ. Sci. Technol.* **1998**, *32*, 1398−1403.
(19) Xiao, Y.; Lasaga, A. C. *Geochim. Cosmochim. Acta* **1994**, *58*, 5379−5400.
(20) Stumm, W. In *Perspectives in Environmental Chemistry*; Macalady, D. L., Ed.; Oxford University Press: Oxford, U.K., 1998; Chapter 1.
(21) Sakanakura, H.; Tanaka, N. *Haikibutsu Gakkai Ronbunshi* **1998**, *9*, 1−10.
(22) Kersten, M.; Förstner, U. In *Chemical Speciation in the Environment*, 1st ed.; Ure, A. M., Davidson, C. M., Eds.; Chapman & Hall: Glasgow, Scotland, 1995; Chapter 9.
(23) Baffi, F.; Ianni, C.; Ravera, M.; Soggia, F.; Magi, E. *Anal. Chim. Acta* **1998**, *360*, 27−34.
(24) Nirel, P. M. V.; Morel, F. M. M. *Water Res.* **1990**, *24*, 1055−1056.
(25) Kheboian, C.; Bauer, C. F. *Anal. Chem.* **1987**, *59*, 1417−1423.
(26) Biester, H.; Scholz, C. *Environ. Sci. Technol.* **1997**, *31*, 233−239.
(27) Ostergren, J. D.; Brown, G. E., Jr.; Parks, G. A.; Tingle, T. N. *Environ. Sci. Technol.* **1999**, *33*, 1627−1636.
(28) Tipping, E.; Hetherington, N. B.; Hilton, J.; Thompson, D. W.; Bowles, E.; Hamilton-Taylor, J. *Anal. Chem.* **1985**, *57*, 1944−1946.
(29) Rendell, P. S.; Batley, G. E.; Cameron, A. J. *Environ. Sci. Technol.* **1980**, *14*, 314−318.
(30) Ho, M. D.; Evans, G. J. *Environ. Sci. Technol.* **2000**, *34*, 1030−1035.
(31) Tessier, A.; Campbell, P. G. C.; Bisson, M. *Anal. Chem.* **1979**, *51*, 844−851.
(32) Murray, K. S.; Cauvet, D.; Lybeer, M.; Thomas, J. C. *Environ. Sci. Technol.* **1999**, *33*, 987−992.
(33) Li, X.; Coles, B. J.; Ramsey, M. H.; Thornton, I. *Chem. Geol.* **1995**, 109−123.
(34) Thöming, J.; Calmano, W. *Acta Hydrochim. Hydrobiol.* **1998**, *26*, 338−343.
(35) Means, J. L.; Smith, L. A.; Nehring, K. W.; Brauning, S. E.; Gavaskar, A. R.; Sass, B. M.; Wiles, C. C.; Mashni, C. I. *The Application of Solidification/Stabilization to Waste Materials*; Lewis Publishers: Boca Raton, FL, 1995.
(36) *Solid Waste, Granular Inorganic Material: Column Leaching Test*; Nordtest: Espoo, Finland, 1995; NT ENVIR 002.
(37) Lide, D. R.; Frederikse, H. P. R. *CRC Handbook of Chemistry and Physics*, 74th ed.; CRC Press: Boca Raton, FL, 1993.

Received for review August 3, 2000. Revised manuscript received December 1, 2000. Accepted December 27, 2000.

ES0001759